1 **Microtubule inhibitors identified through non-biased screening**

2 **enhance DNA transfection efficiency by delaying p62-dependent**

3 **ubiquitin recruitment**

4

5 Megumi Tsuchiya[1#], Hidesato Ogawa[1#]*, Kento Watanabe[1], Takako Koujin[2], Chie

6 Mori[2], Kazuto Nunomura[3], Bangzhong Lin[3], Akiyoshi Tani[3], Yasushi Hiraoka[1,2], and

7 Tokuko Haraguchi[1,2]*

8

9 [1]Graduate School of Frontier Biosciences, Osaka University, 1-3 Yamadaoka, Suita

10 565-0871, Japan

11 [2]Advanced ICT Research Institute Kobe, National Institute of Information and

12 Communications Technology, 588-2 Iwaoka, Iwaoka-cho, Nishi-ku, Kobe 651-2492,

13 Japan

14 [3]Graduate School of Pharmaceutical Science, Osaka University, 1-6 Yamadaoka, Suita

15 565-0871, Japan

16 # These authors contributed equally to this manuscript.

17

18 *Correspondence should be addressed to:

19 Hidesato Ogawa, Tel: +81 668794621; Fax: +81 668794622

20 E-mail address: hidesato@fbs.osaka-u.ac.jp

21 Tokuko Haraguchi, Tel: +81 668794621; Fax: +81 668794622

22 E-mail address: haraguchi@fbs.osaka-u.ac.jp

23 **Short title**: MT drugs enhance transfection efficiency

Abstract

Ectopic gene expression is an indispensable tool in biology and medicine, but is often limited by the low efficiency of DNA transfection. We previously reported that depletion of the autophagy receptor p62/SQSTM1 enhances DNA transfection efficiency by preventing the degradation of transfected DNA. Therefore, p62 is a potential target for drugs to increase transfection efficiency. To identify such drugs, a non-biased high-throughput screening was applied to over 4,000 compounds from the Osaka University compound library, and their p62-dependency was evaluated. The top-scoring drugs were mostly microtubule inhibitors, such as colchicine and vinblastine, and all of them showed positive effects only in the presence of p62. To understand the p62-dependent mechanisms, the time required for p62-dependent ubiquitination, which is required for autophagosome formation, was examined using polystyrene beads that were introduced into cells as materials that mimicked transfected DNA. Microtubule inhibitors caused a delay in ubiquitination. Furthermore, the level of phosphorylated p62 at S405 was markedly decreased in the drug-treated cells. These results suggest that microtubule inhibitors inhibit p62-dependent autophagosome formation. Our findings demonstrate for the first time that microtubule inhibitors suppress p62 activation as a mechanism for increasing DNA transfection efficiency and provide solutions to increase efficiency.

Keywords: high-throughput screening; transfection efficiency; autophagy; p62; phosphorylation; ubiquitination; gene delivery

Introduction

Gene delivery is one of the most important steps in gene therapy and genetic modification in basic science. Gene therapy has great potential in clinical medicine, and this concept has become well established in therapeutic approaches. In basic science, DNA transfection is a powerful tool that enables the study of gene functions and their products in cells.

Endocytosis is a crucial pathway for the regulation of cellular uptake of plasmid DNA (Rejman *et al.* 2005; Khalil *et al.* 2006; Midoux *et al.* 2008). Importantly, endocytosis can promote the induction of selective autophagy, also called xenophagy (Chen *et al.* 2014). Generally, autophagy is a cytosolic bulk degradation pathway for the recycling of biomolecules through nonspecific degradation of proteins and organelles under nutrient starvation conditions. In contrast, selective autophagy plays an important defensive role against cellular infection by pathogens, as part of a starvation-independent autophagic defense system (Nakatogawa *et al.* 2009; Mizushima *et al.* 2011; Galluzzi *et al.* 2017). The conjugation of ubiquitin (Ub) to target pathogens is an important initial process in selective autophagy. Ubiquitination assists in the recruitment of autophagy receptor proteins, including p62/sequestosome-1 (p62/SQSTM1), against pathogens or transfected DNA (Dupont *et al.* 2010; Roberts *et al.* 2013; Chen *et al.* 2014; Alomairi *et al.* 2015; Tsuchiya *et al.* 2016). Therefore, suppression of the autophagy pathway can be a target for drugs to increase transfection efficiency.

We have previously reported that the depletion of the p62/SQSTM1 protein (hereafter designated p62) greatly increases the efficiency of DNA transfection in cultured cells (Tsuchiya *et al.* 2016). To monitor the behavior of the transfected DNA, we developed an experimental system using DNA-conjugated beads that mimic the

3

71   transfected DNA. In this system, DNA-conjugated beads together with pHrodo, a

72   fluorescent marker for endosome rupture, were incorporated into cells, and their

73   intracellular dynamics were analyzed in a live cell (Tsuchiya *et al.* 2016). Using this

74   system, we demonstrated that the transfected DNA was incorporated into cells through

75   endocytosis, released from the endosomes into the cytosol, and entrapped via autophagy

76   in a p62-dependent manner. Furthermore, we demonstrated that the recruitment of Ub

77   around the transfected material was significantly delayed in p62 gene-knockout murine

78   embryonic fibroblast (p62KO-MEF) cells compared with that in normal MEF cells

79   (Tsuchiya *et al.* 2018). Additionally, p62 phosphorylation at S405 (equivalent to human

80   S403) is a crucial step for the recruitment of Ub to the target site of transfected materials

81   that mimic ectopic DNA (Tsuchiya *et al.* 2016). Hence, p62 phosphorylation at S405 is

82   an essential step for transfection-induced selective autophagy (Tsuchiya *et al.* 2018). As

83   p62 plays an important role in gene delivery through initial ubiquitination of the

84   transfected DNA, inhibition of p62 may increase transfection efficiency. The aim of this

85   study was to identify a small chemical compound that blocks the initial step of p62-

86   dependent selective autophagy to enhance DNA transfection efficiency in mammalian

87   cells.

88

89   **Results**

90   **High-throughput screening for drugs enhancing transfection efficiency**

91   To identify potential compounds that can enhance transfection efficiency, high-

92   throughput screening based on a luciferase assay was performed on MEF cells using an

93   automated workstation (Fig. 1A). The MEF cells were seeded in 384-well plates and

94   incubated for 18 h with each compound from the Osaka University compound library

4

95   (4,400 compounds; Tachibana *et al.* 2018) at a final concentration of 10 µM. The

96   negative control was dimethyl sulfoxide (DMSO) at a final concentration of 1%. The

97   cells were transfected with the pCMV-Luc plasmid (encoding luciferase driven by the

98   cytomegalovirus immediate early (CMV-IE) promoter) for 28 h using Lipofectamine

99   2000. The cells were subjected to a cell viability assay, followed by a luciferase assay

100   (Fig. 1A). Luciferase activity, as expressed from the transfected plasmid, was measured,

101   and transfection efficiency was evaluated based on luciferase activity normalized to cell

102   viability. Among the 4,400 compounds tested, 160 were removed from the list for

103   selection as valid compounds because of severe defects in cell morphology. The

104   transfection efficiency of the cells treated with each of the remaining 4,240 compounds

105   is plotted in Fig. 1B. In this first screening, out of the 4,240 tested compounds, we

106   identified 87 compounds that increased luciferase activity compared with that in the

107   negative control (approximately 2.1% positive hit rate). The cutoff value used for

108   selection was the mean value of the DMSO control + 4 × standard deviation (SD) (mean

109   0.347, SD = 0.242).

110   The activities of these 87 compounds were further analyzed via a second

111   screening. To achieve this, MEF cells were cultured in 96-well plates and transfected

112   with the pCMV-Luc plasmid for 28 h using Lipofectamine 2000 in the presence of each

113   of these compounds at a concentration of 1 µM (Fig. 2A). Transfection efficiency was

114   determined by a luciferase assay, in which luciferase activity expressed from the

115   transfected plasmid was measured and normalized to cell viability, as described in

116   Experimental procedures. The transfection efficiency values for the 87 compounds are

117   listed in Table S1. Notably, the top 9 compounds with high transfection efficiencies (>

118   20-fold that of the negative control) were all microtubule inhibitors (Fig. 2B; Table S1).

119   As microtubule inhibitors were found to increase transfection efficiency, we

120   also tested nocodazole, an extensively used microtubule inhibitor, which was not

121   included in the Osaka University compound library. Transfection efficiency was

122   determined in the presence or absence of 1 μM nocodazole in 96-well plates (Fig. S1).

123   The results show that nocodazole has a transfection-enhancing activity at 1 μM, similar

124   to colchicine (Fig. S1).

125   We further examined whether microtubule inhibitors are effective against

126   various transfection reagents with different mechanisms. Effectene (a non-liposomal

127   lipid reagent) and Viofectin (a non-lipid high-charge cationic polymer reagent) were

128   examined in addition to the previously used Lipofectamine 2000 (a cationic lipid

129   reagent). In the presence of 300 nM colchicine, the transfection efficiencies in all these

130   transfection reagents increased, although the degree of effectiveness varied (Fig. S2).

131   The increase in transfection efficiency in the presence of 300 nM colchicine was

132   approximately 2-, 6-, and 29-fold in Effectene, Viofectin, and Lipofectamine 2000,

133   respectively (Fig. S2), suggesting that colchicine is effective with various non-viral

134   transfection reagents.

135

136   **Microtubule inhibitors enhance gene transfection efficiency**

137   To further evaluate the effects of microtubule inhibitors on DNA transfection efficiency,

138   we selected two commonly used microtubule inhibitors, colchicine and vinblastine.

139   These were ranked second and third, respectively, in the 2nd screening (Fig. 2A). First,

140   we examined the dose-dependency of these inhibitors in MEF cells (Fig. 2C). Cells

141   were treated with colchicine or vinblastine at various concentrations and transfected

142   with the pCMV-Luc DNA plasmid. Then, their luciferase activity was measured to

143   determine transfection efficiency. Transfection efficiency increased in a dose-dependent

144   manner in the MEF cells (Fig. 2C). Statistical analysis showed that the EC50 (half-

145   maximal effective concentration) of colchicine and vinblastine was 239.1 and 26.29 nM,

146   respectively, in the MEF cells (Fig. 2C). Furthermore, we evaluated transfection

147   efficiency by observing GFP expression in MEF cells. The number of GFP-positive

148   cells was greater in colchicine- and vinblastine-treated cells than in DMSO-treated

149   control cells, and cell viability was approximately 70% in both drug-treated cells

150   compared with that in the control under these conditions (Fig. 2D). These results

151   suggest that treatment with colchicine and vinblastine can enhance transfection

152   efficiency.

153   As microtubule depolymerization activates the transcription factor NF-κB to

154   induce NF-κB-dependent gene expression (Rosette & Karin, 1995) and the CMV

155   promoter in the pCMV-Luc plasmid possesses an NF-κB binding site (Rosette & Karin,

156   1995; Wang & MacDonald, 2004), treatment with microtubule inhibitors may induce

157   luciferase gene expression through NF-κB-mediated CMV promoter activation. To

158   eliminate this possibility, we tested promoter activity in a cell line (MEF-LUC cells)

159   with a CMV-driven luciferase plasmid integrated into the genome. In these cells, we

160   measured the levels of luciferase activity in the presence or absence of colchicine or

161   vinblastine. Treatment with colchicine for 27 h increased luciferase gene expression

162   only marginally (approximately 1.2-fold), which did not explain the considerably

163   greater increase (approximately 40-fold) in the transfected DNA plasmids (Fig. S3A;

164   compare with Fig. 2C). Treatment with vinblastine also yielded a similar result, with

165   almost no increase in luciferase expression (Fig. S3B; compare with Fig. 2C). These

166   results indicate that the increase in transfection efficiency in the presence of microtubule

167   inhibitors does not reflect NF-κB-dependent promoter activation.

168

169   **Transfection enhancement occurs in the presence of autophagy receptor p62**

170   As p62 acts as an inhibitory factor for DNA transfection by recruiting LC3

171   (microtubule-associated protein 1A/1B-light chain 3; also called ATG8), a marker

172   protein for autophagosomes, to transfected DNA (Tsuchiya *et al.* 2016), the

173   transfection-enhancing activity of the tested compounds may be deduced by the

174   invalidation of the p62-dependent autophagic pathway. Based on this hypothesis, we

175   examined the activity of the 87 compounds at a concentration of 1 μM in p62KO-MEF

176   cells under the same conditions as those in Fig. 2A (Fig. 3A). All compounds exhibited

177   little or no transfection-enhancing activity in p62KO-MEF cells (Fig. 3A). As the

178   microtubule inhibitors (compounds 1–9 in Fig. 2B) seemed to show a slight increase in

179   transfection enhancing activity (Fig. 3A), we further tested colchicine and vinblastine

180   for transfection-enhancing activity at various concentrations from 15.6 to 2000 nM (Fig.

181   3B, C) and found that these two microtubule inhibitors did not show transfection-

182   enhancing activity at any of the tested concentrations (Fig. 3B, C). This result suggests

183   that microtubule inhibitors function in a p62-dependent autophagic pathway.

184

185   **p62-dependent ubiquitination is delayed by microtubule inhibitors**

186   To understand the molecular mechanisms of the p62-dependent enhancement of

187   transfection efficiency by colchicine and vinblastine, we employed an experimental

188   method using polystyrene beads that had been developed to monitor the behavior of the

189   transfected DNA (Kobayashi *et al.* 2010) (Fig. 4A). In this method, the beads are

8

190   incorporated into cells with transfection reagents via endocytosis and enter the cytosol

191   after rupture of the endosomal membrane. The beads that appeared in the cytosol were

192   targeted for autophagy, similar to the transfected DNA (Kobayashi *et al.* 2010;

193   Kobayashi *et al.* 2015) (Fig. 4A). For monitoring in living cells, the beads were pre-

194   conjugated with pHrodo dye, which emits fluorescence under acidic pH conditions,

195   such as those in the acidic endosome but not in the cytosol. Therefore, this dye serves as

196   a marker of endosome membrane rupture, as previously described (Kobayashi *et al.*

197   2010). The pHrodo-conjugated beads were incorporated into MEF cells expressing

198   GFP-fused Ub protein (GFP-Ub MEF cells) (Tsuchiya *et al.* 2018), and the assembly of

199   GFP-Ub around the beads was observed in a living cell using time-lapse fluorescence

200   microscopy (Fig. 4B). In the control DMSO-treated cells, the time for Ub recruitment to

201   the beads was approximately 3–4 min (Fig. 4B, middle panel) after the disappearance of

202   pHrodo fluorescence (Fig. 4B, upper panel). In contrast, the time for GFP-signal

203   accumulation was 9–10 min in 500 nM colchicine-treated MEF cells (Fig. 4C, middle

204   panel), which was longer than that in the control cells (Fig. 4B). Statistical analysis was

205   performed to determine the timing of GFP-signal accumulation around the beads after

206   the loss of pHrodo signals in cells expressing GFP-Ub with or without the inhibitor

207   (Fig. 4D). In the DMSO-treated cells, the time for Ub recruitment to the beads was ~4

208   min (median) after the disappearance of pHrodo fluorescence (mean and SD, $4.167 \pm$

209   1.88 min, $n = 24$ beads; lane 1 in Fig. 4D). Moreover, the timing of GFP-signal

210   accumulation was ~6 min (median) in the 100 nM colchicine-treated MEF cells (mean

211   and SD: 8.286 ± 8.36 min, $n = 28$ beads: lane 2 in Fig. 4D), ~11 min (median) in the

212   500 nM colchicine-treated MEF cells (mean and SD: 11.32 ± 11.30 min, $n = 22$ beads:

213   lane 3 in Fig. 4D), and ~6 min (median) in the vinblastine-treated MEF cells (mean and

9

214   SD: 6.48 ± 3.81 min, *n* = 31 beads; lane 4 in Fig. 4D). Additionally, the GFP-Ub signals

215   did not accumulate within 60 min in colchicine- or vinblastine-treated GFP-Ub MEF

216   cells (these beads were not counted and were not included in the *n*; upper column in Fig.

217   4D). These results show that GFP-Ub accumulation around the beads was significantly

218   delayed in colchicine- or vinblastine-treated MEF cells. Colchicine and vinblastine have

219   different effects on microtubule depolymerization; colchicine forms diffusely

220   distributed tubulins/microtubules, whereas vinblastine forms the paracrystal structure of

221   the microtubules (Haraguchi *et al.* 1997). Nonetheless, both have the same function of

222   increasing DNA transfection efficiency, suggesting that normal microtubule function or

223   structure is important for Ub recruitment to the target site.

224

225   **Active form of p62 is suppressed by microtubule inhibitors**

226   It has been reported that the phosphorylated form of p62 at amino acid residue S405

227   (p62 S405) is required for Ub recruitment during selective autophagy (Tsuchiya *et al.*

228   2018). Therefore, Ub recruitment can be delayed by a decrease in the level of

229   phosphorylated p62 at S405. To test this hypothesis, we performed Western blot

230   analysis to evaluate the total p62 protein levels and p62 S405 phosphorylation levels

231   (Fig. 5). The p62 S405 phosphorylation levels were very low before DNA transfection

232   ("no transfection" in Fig. 5). However, after transfection ("DNA transfection 24 h"),

233   these levels greatly increased in DMSO-treated MEF cells, although the p62 levels

234   remained unchanged. This suggests that DNA transfection induced an increase in p62

235   S405 phosphorylation. However, in MEF cells treated with colchicine or vinblastine,

236   the level of p62 S405 phosphorylation decreased. This suggests that microtubule

237   inhibitors inhibit Ub recruitment by decreasing the level of phosphorylated p62 at S405.

10

238

Discussion

Microtubule structure/function and transfection efficiency

241 In this study, we used a non-biased, high-throughput screening approach to identify

242 small chemical compounds that increase DNA transfection efficiency and identified

243 microtubule inhibitors as the top 9 compounds. Therefore, inhibition of the microtubule

244 structure or function seems to trigger an increase in transfection efficiency. This finding

245 is consistent with previous reports that microtubule depolymerizing reagents,

246 nocodazole, increased transfection efficiency in CV-1 cells (Lindberg *et al.* 2001) and

247 colchicine and vinblastine increased transfection efficiency in cultured vascular smooth

248 muscle cells (Wang & MacDonald 2004). Additionally, microtubule-polymerizing

249 reagents, such as paclitaxel, also increase the transfection efficiency in COS-7 and A549

250 cells (Hasegawa *et al.* 2001; Nair *et al.* 2002). The polymerizing agent docetaxel, a

251 chemical compound closely related to paclitaxel, was included in our screening results

252 for the top 9 compounds (Fig. 2B, Rank 7). Moreover, tubulin deacetylation inhibitors,

253 such as HDAC6 inhibitors, also increase transfection efficiency in A549 cells, PC3

254 cells, and mesenchymal stem cells (Vaughan *et al.* 2008; Barua & Rege 2010; Ho *et al.*

255 2017). This is likely because acetylated tubulin can stabilize microtubule structures,

256 which in turn implies that microtubule structure stabilization can also increase gene

257 transfection efficiency. Taken together, these findings strongly suggest that inhibition of

258 the intact structure or dynamic nature of microtubules is important for increasing the

259 efficiency of gene transfection.

260

Microtubule inhibitors affect selective autophagy pathways

262   Our results showed that treatment of cells with colchicine or vinblastine increased

263   transfection efficiency in a p62-dependent manner. However, it is difficult to attribute

264   these observations to a particular cause. Microtubules are major contributors to the

265   trafficking of several components in the endosomal/lysosomal pathway; hence, it is

266   logical to propose that these inhibitors may block the autophagy pathway. The role of

267   microtubules in autophagosome formation appears to be different based on the culture

268   medium conditions, e.g., vegetatively growing medium (basal) or starvation medium

269   (inducible) conditions. Several studies have used microtubule inhibitors under basal

270   conditions to show that microtubules do not participate in autophagosome formation

271   (Reunanen *et al.* 1988; Aplin *et al.* 1992; Kochl *et al.* 2006). However, under inducible

272   conditions, disassembling the microtubules with these inhibitors prevented

273   autophagosome formation, suggesting that microtubules play a crucial role in this

274   process (Kochl *et al.* 2006; Geeraert *et al.* 2010). Previous studies have shown that

275   transfected DNA also induces the selective autophagy pathway (Roberts *et al.* 2013;

276   Chen *et al.* 2014; Tsuchiya *et al.* 2016); hence, microtubule inhibitors may affect

277   transfection-induced autophagosome formation. The detailed mechanisms of the

278   inhibition of autophagosome formation following microtubule inhibitor treatment are

279   not clear; however, several autophagy factors are associated with microtubules,

280   including ATG8 (LC3), ATG1 (ULK1), ATG6 (Beclin1), ATG18 (WIPI1), and p62

281   (Mackeh *et al.* 2013). LC3 has long been thought to be involved in the regulation of

282   microtubule assembly and disassembly (Mann & Hammarback 1994; Deretic 2008).

283   Furthermore, ATG18-positive pre-autophagosomal structures can move along

284   microtubules, and this movement is extremely sensitive to microtubule inhibitor

285   treatment (Polson *et al.* 2010). These data suggest that microtubules contribute to the

12

286   sequestration, recruitment, and movement of autophagy factors for the formation of

287   inducible autophagosomes. Therefore, microtubule inhibitors may block the inducible

288   autophagy pathway, resulting in a decrease in the likelihood of DNA degradation and

289   increase in transfection efficiency.

290

291   **Microtubule inhibitors decrease the level of phosphorylated p62**

292   The ubiquitination of endosome membrane proteins surrounding exogenous material,

293   such as transfected DNA, is the initial step in inducible selective autophagy (Randow

294   2011; Wileman 2013; Tsuchiya *et al.* 2016). In our study, treatment with colchicine or

295   vinblastine delayed the recruitment of Ub proteins. This delay in recruitment is also

296   caused by the depletion of p62 or mutation of the p62 phosphorylation site at S405

297   (human S403) (Tsuchiya *et al.* 2018). As p62 has been reported as a microtubule-

298   associated factor (Geeraert *et al.* 2010), treatment with a microtubule inhibitor may

299   affect p62-mediated Ub recruitment. Specifically, our results showed that p62 S405

300   phosphorylation was significantly impaired by treatment with colchicine or vinblastine

301   after transfection. p62 S405 is phosphorylated by kinases such as CK2 and TBK1

302   (Matsumoto *et al.* 2011; Matsumoto *et al.* 2015). These kinases are also associated with

303   tubulin (Faust *et al.* 1999; Lim *et al.* 2004; Pillai *et al.* 2015; Yang *et al.* 2018). After

304   transfection, the recruitment of these kinases may be affected by treatment with

305   microtubule inhibitors. Further studies are necessary to elucidate the detailed

306   mechanisms by which these microtubule inhibitors affect the phosphorylation levels of

307   p62.

308   In this study, a non-biased high-throughput screening method revealed that

309   microtubule inhibitors are the most effective reagents for increasing transfection

310   efficiency among the drugs present in the Osaka University compound library, and

311   revealed for the first time, the mechanism by which microtubule inhibitors increase

312   transfection efficiency; that is, microtubule inhibitors suppress p62 phosphorylation,

313   which is required for autophagosome formation to degrade transfected DNA. Our

314   findings provide solutions to increase transfection efficiency.

315

316   **Experimental procedures**

317   **Plasmids**

318   pCMV-Luc plasmid encoding the luciferase gene *luc2*, used as a luciferase expression

319   vector in this study, was purchased from Promega (E1310; pGL4.50 [*luc2*/CMV/Hygro]

320   vector; Promega, Madison, WI, USA). The GFP expression plasmid pCMX-AFAP was

321   prepared as previously described (Ogawa *et al.* 2004).

322   To create cells stably expressing luciferase (see the next section), we constructed

323   the PB-CMV-LUC-Zeo vector. We first constructed the PB-EF1-MCS-IRES-Zeo

324   vector. To insert the zeocin resistance gene DNA sequence, two DNA fragments (#1

325   and #2) were amplified as follows: the cloning site with Kozak sequence fragment #1

326   was amplified from the PB-EF1-MCS-IRES-Neo vector (PB533A-2; System

327   Biosciences, Palo Alto, CA, USA) using PCR and the following primers: 5′-

328   CTGAAGGATGCCCAGAAGGTACCCCATTGT-3′ and 5′-

329   TCCGGACGCCATGGTTGTGG-3′. The zeocin coding fragment #2 was amplified

330   from the pcDNA3.1/Zeo (+) vector (V86020; Thermo Fisher Scientific, Yokohama,

331   Japan) using PCR and the following primers: 5′-

332   ACAACCATGGCGTCCGGAATGGCCAAGTTGACCAGTGCCGTTCC-3′ and 5′-

333   TCCAGAGGTTGATTGTCGACTCAGTCCTGCTCCTCGGCCACGAA-3′.

14

334   Following digestion with KpnI and SalI, fragments #1 and #2 were inserted into the PB-

335   EF1-MCS-IRES-Neo vector using the In-Fusion HD Cloning Kit (639648; Takara Bio

336   Inc. Kusatsu, Japan). This resulted in the PB-EF1-MCS-IRES-Zeo vector. Next, the

337   human cytomegalovirus immediate early enhancer and promoter (CMV-IE) DNA

338   sequence (#3) was amplified from the pGL4.50 [*luc2*/CMV/Hygro] vector using PCR

339   and the following primers: 5′-

340   GGGGATACGGGGAAAAGGCCTCGTTACATAACTTACGGTAAATG-3′ and 5′-

341   GAATTCGCTAGCTCTAGAAGCTCTGCTTATATAGACCTCCCACC-3′. The

342   luciferase DNA sequence (#4) was amplified from the pGL4.50 [*luc2*/CMV/Hygro]

343   vector using PCR and the following primers: 5′-

344   TCTAGAGCTAGCGAATTCATGGAAGATGCCAAAAACATTAAGAA-3′ and 5′-

345   CGATTTAAATTCGAATTCTTACACGGCGATCTTGCCGCCCTTCT-3′. Following

346   digestion with EcoRI and StuI, fragments #3 and #4 were inserted into the PB-EF1-

347   MCS-IRES-Zeo vector using the In-Fusion HD Cloning Kit. This resulted in the PB-

348   CMV-LUC-Zeo vector.

349

350   **Cell strains**

351   p62KO-MEF cells (p62$^{-/-}$ cells) and their parental MEF cells were kindly provided by

352   Dr. Tetsuro Ishii (University of Tsukuba) (Komatsu *et al.* 2007). MEF cells stably

353   expressing GFP-Ub were generated as previously described (Tsuchiya *et al.* 2018). To

354   obtain MEF cells or p62KO-MEF cells stably expressing luciferase, MEF cells or

355   p62KO-MEF cells were transfected with the PB-CMV-LUC-Zeo plasmid (generated as

356   described in the previous section) and cultured in the presence of 100 μg/mL Zeocin

357   (R25501, Thermo Fisher Scientific), and then, single clones (MEF-LUC cells) were

358   selected. Each stable clone was examined for luciferase protein expression using a

359   luciferase assay.

360

361   **Cell culture**

362   All cell lines were maintained in culture medium (Dulbecco's modified Eagle medium

363   (DMEM) (D6429; Sigma-Aldrich, St. Louis, MO, USA) supplemented with 10% fetal

364   bovine serum) in the presence of 5% CO_2 at 37°C.

365

366   **High-throughput screening for enhancer compounds**

367   The MEF cells were seeded at a density of 0.8×10^3 cells per well (384-well microplate,

368   781091; Greiner Bio-One, Tokyo, Japan) using a Multidrop COMBI (Thermo Fisher

369   Scientific) and cultured for 6 h in culture medium. The cells were pretreated for 18 h

370   with 1% DMSO (negative control) or the screening compounds (10 μM each) using a

371   Fluent780® Automation Workstation (Tecan Japan, Kawasaki, Japan) with a 96-

372   channel head adapter and Tecan sterile tips (30048824; Tecan Japan). The pretreated

373   cells in each well were transfected with 25 ng of pCMV-Luc plasmid using

374   Lipofectamine 2000 (Thermo Fisher Scientific) for 28 h in the presence of each

375   compound. Cell viability was measured with the RealTime-Glo™ MT Cell Viability

376   Assay (E9713; Promega) using the GloMax® Discover Microplate Reader (Promega).

377   Luciferase activity was measured with the ONE-Glo™ Luciferase Assay System

378   (E6120; Promega) using the GloMax® Discover Microplate Reader according to the

379   manufacturer's protocol. The values of luciferase activity were normalized to the cell

380   number obtained from cell viability measurements.

381

16

Transfection efficiency measurements

Transfection efficiency was determined based on the luciferase activity expressed from the transfected plasmid. Cells were seeded at a density of 0.45×10^4 cells per well (96-well assay plate; 3603 Corning, Corning, NY, USA) and cultured overnight in culture medium. The cells were pretreated with 1% DMSO (negative control) or the screening compounds (0.1–10 μM each) for 30 min. The cells were then transfected with 100 ng of pCMV-Luc plasmid using Lipofectamine 2000 for 28 h in the presence of each compound. Cell viability was measured with the RealTime-Glo™ MT Cell Viability Assay using the GloMax® 96 Microplate Luminometer (Promega). Luciferase activity was measured with the ONE-Glo™ Luciferase Assay System using the GloMax® 96 Microplate Luminometer according to the manufacturer's protocol. The values of luciferase activity were normalized to the cell number obtained from cell viability measurements. Mean EC50 values and SDs were determined from three independent experiments. Transfection efficiencies were determined by luciferase activity normalized to cell viability.

Viofectin (VFT1001; Viogene, Nacalai tesque, Kyoto, Japan) and Effectene (301425; Qiagen, Tokyo, Japan) were also used as transfection reagents. For Viofectin, the same transfection procedure as that described above for Lipofectamine 2000 was used, except that the reagents were different. For Effectene, some procedures were modified as follows: initial cell density was 1×10^4 cells per well and the cells were transfected for 4 h and further incubated for another 20 h in culture medium without transfection reagents.

GFP expression

17

406   MEF cells were seeded at a density of 1.5×10^5 cells per well (6-well assay plate; 3335

407   Corning, Corning, NY, USA) and cultured overnight in culture medium. The cells were

408   pretreated with 1% DMSO (negative control), 250 nM cholchicine, or 50 nM

409   vinblastine for 30 min. The cells were then transfected with 2 μg of pCMV-Luc plasmid

410   using Lipofectamine 2000 for 24 h in the presence of each drug. The cells were

411   observed using an objective lens (N Plan 5x/0.12 PH 0) on a Leica DM IL LED

412   fluorescence microscope (Leica Microsystems, Wetzlar, Germany).

413

414   **Preparation of pHrodo-conjugated beads**

415   pHrodo-conjugated beads were prepared as previously described (Kobayashi *et al.*

416   2010). Briefly, Dynabeads M-270 Streptavidin (DB65306; Thermo Fisher Scientific)

417   were washed three times with phosphate buffered saline (PBS) and resuspended in 100

418   mM sodium bicarbonate buffer (pH 8.5) to an appropriate concentration (typically a

419   1:10 or 1:20 dilution). pHrodo-succinimidyl ester (P36600; Thermo Fisher Scientific)

420   was then added to the bead suspension and incubated in sodium bicarbonate buffer for 1

421   h at room temperature (about 26°C). After the conjugation reaction, the beads were

422   washed with sodium bicarbonate buffer and suspended in PBS.

423

424   **Incorporation of beads into living cells**

425   One day before incorporating the beads, GFP-Ub MEF cells were seeded onto 35 mm

426   glass-bottom culture dishes (P35G-1.5-10-C; MatTek, Ashland, MA, USA) at a density

427   of 1.5×10^5 cells/dish in culture medium. The cells were pretreated with each

428   microtubule inhibitor (100 nM colchicine, 500 nM colchicine, or 100 nM vinblastine) or

429   DMSO as a control for 30 min at 37°C in a CO_2 incubator before bead incorporation.

18

430   The transfection reagent Effectene (301425; Qiagen, Tokyo, Japan) was used to

431   incorporate the beads. Transfection-reagent-coated beads were prepared by mixing

432   pHrodo-conjugated beads with the Effectene transfection reagent according to the

433   manufacturer's protocol, except that a bead suspension was used instead of the DNA

434   solution. The resulting bead mixture (~10 μL) was mixed with 90 μL of the culture

435   medium containing each microtubule inhibitor and added to the cells by replacing the

436   medium. After incubation for 1 h at 37°C in a CO_2 incubator, the cells were washed

437   twice with fresh growth medium to remove unattached beads and then further incubated

438   with the medium containing each microtubule inhibitor or control DMSO for the time

439   indicated in each experiment.

440

441   **Time-lapse imaging**

442   Cells were treated with 100 ng/mL Hoechst 33342 (B2261; Sigma-Aldrich) for 15 min

443   to stain chromosomes, as previously described (Haraguchi *et al.* 1997), except that the

444   medium containing each microtubule inhibitor or control DMSO was used. After

445   washing with the culture medium, the cells were cultured in fresh culture medium

446   (phenol red-free DMEM containing 10% fetal bovine serum) containing each

447   microtubule inhibitor or control DMSO. Time-lapse observations were performed using

448   an oil-immersion objective lens (UApo40/NA1.35; Olympus, Tokyo, Japan) on a

449   DeltaVision microscope system (GE Healthcare Life Sciences Japan, Tokyo, Japan)

450   placed in a temperature-controlled room (37°C), as previously described (Haraguchi *et*

451   *al.* 1997). Images were obtained every minute for approximately 60 min.

452   The timing of GFP-Ub fluorescence signal accumulation around the beads was

453   determined as previously described (Tsuchiya *et al.* 2018). Briefly, the fluorescence

19

454   intensity of the region (18 pixels square) surrounding the beads was measured using the

455   FUJI software suite (IMAGE J; National Institutes of Health, Bethesda, MD, USA), and

456   the background fluorescence intensity of the region with no beads in the same cell was

457   subtracted.

458

459   **Western blot analysis**

460   MEF cells were seeded at a density of 1.5×10^5 cells per well (6-well assay plate; 3335

461   Corning, Corning, NY, USA) and cultured overnight in culture medium. The cells were

462   pretreated with 1% DMSO (negative control), 500 nM colchicine, or 100 nM

463   vinblastine for 30 min. The cells were then transfected with 2 μg of pCMX-AFAP

464   plasmid using Lipofectamine 2000 for 24 h in the presence of each drug. Western blot

465   analysis was performed as previously described (Tsuchiya *et al.* 2018). Briefly, cell

466   lysates were prepared in a lysis buffer [50 mM Tris-HCl, pH 7.5, 150 mM NaCl, 1 mM

467   EDTA, 1% Triton X-100, 1 x Phosphatase Inhibitor Cocktail Solution Ⅱ (160-24371;

468   FUJIFILM Wako Pure Chemical Corporation, Osaka, Japan) and 1 x protease inhibitor

469   cocktail (Nacalai tesque Inc., Kyoto, Japan)]. The lysates were subjected to

470   electrophoresis on NuPAGE 4% to 12% Bis-Tris gels (NP0321; Thermo Fisher

471   Scientific). Proteins were transferred to polyvinylidene fluoride membranes and probed

472   using anti-p62 (SQSTM1) (PM045; MBL, Nagoya, Japan), anti-Phospho-

473   SQSTM1/p62(Ser403) (D8D6T; Cell Signaling Technology, Danvers, MA, USA), and

474   anti-glyceraldehyde 3-phosphate dehydrogenase (GAPDH) (14C10; Cell Signaling

475   Technology) antibodies, and secondary antibody conjugated to horseradish peroxidase

476   (NA9340V; GE Healthcare Life Sciences). Protein bands were stained with

20

477   ImmunoStar Zeta (295-72404; FUJIFILM Wako Pure Chemical Corporation) and

478   detected by chemiluminescence using a ChemiDoc MP imaging system (Bio-Rad,

479   Tokyo, Japan).

480

481   **Statistical analysis**

482   The *p*-values were obtained by performing Kruskal-Wallis tests using GraphPad Prism

483   8 software (GraphPad Software, Inc., La Jolla, CA, USA).

484

496

497   **Author contributions**

498   MT, HO, KW, TK, CM, KN, BL and AT performed the experiments. MT, HO, AT,

499   YH, and TH designed the experiments. All authors analyzed and discussed the data, and

500   MT, HO, YH, and TH wrote the manuscript.

501

502   **Conflict of interest**

503   All authors declare that: (i) no support, financial or otherwise, has been received from

504   any organization that may have an interest in the submitted work; and (ii) there are no

505   other relationships or activities that could appear to have influenced the submitted work.

References

Alomairi, J., Bonacci, T., Ghigo, E. & Soubeyran, P. (2015) Alterations of host cell ubiquitination machinery by pathogenic bacteria. *Frontiers in cellular and infection microbiology* **5**, 17. https://doi.org/10.3389/fcimb.2015.00017

Aplin, A., Jasionowski, T., Tuttle, D.L., Lenk, S.E. & Dunn, W.A., Jr. (1992) Cytoskeletal elements are required for the formation and maturation of autophagic vacuoles. *J Cell Physiol* **152**, 458-466. https://doi.org/10.1002/jcp.1041520304

Barua, S. & Rege, K. (2010) The influence of mediators of intracellular trafficking on transgene expression efficacy of polymer-plasmid DNA complexes. *Biomaterials* **31**, 5894-5902. https://doi.org/10.1016/j.biomaterials.2010.04.007

Chen, X., Khambu, B., Zhang, H., Gao, W., Li, M., Chen, X., Yoshimori, T. & Yin, X.M. (2014) Autophagy induced by calcium phosphate precipitates targets damaged endosomes. *Journal of Biological Chemistry* **289**, 11162-11174. https://doi.org/10.1074/jbc.m113.531855

Deretic, V. (2008) Autophagosome and phagosome. *Methods Mol Biol* **445**, 1-10. https://doi.org/10.1007/978-1-59745-157-4_1

Dupont, N., Temime-Smaali, N. & Lafont, F. (2010) How ubiquitination and autophagy participate in the regulation of the cell response to bacterial infection. *Biology of the Cell* **102**, 621-634. https://doi.org/10.1042/BC20100101

Faust, M., Schuster, N. & Montenarh, M. (1999) Specific binding of protein kinase CK2 catalytic subunits to tubulin. *FEBS letters* **462**, 51-56. https://doi.org/10.1016/S0014-5793(99)01492-1

Galluzzi, L., Baehrecke, E.H., Ballabio, A. *et al.* (2017) Molecular definitions of autophagy and related processes. *The EMBO journal* **36**, 1811-1836. https://doi.org/10.15252/embj.201796697

Geeraert, C., Ratier, A., Pfisterer, S.G., Perdiz, D., Cantaloube, I., Rouault, A., Pattingre, S., Proikas-Cezanne, T., Codogno, P. & Pous, C. (2010) Starvation-induced hyperacetylation of tubulin is required for the stimulation of autophagy by nutrient deprivation. *J Biol Chem* **285**, 24184-24194. https://doi.org/10.1074/jbc.M109.091553

536 Haraguchi, T., Kaneda, T. & Hiraoka, Y. (1997) Dynamics of chromosomes and
537   microtubules visualized by multiple-wavelength fluorescence imaging in living
538   mammalian cells: effects of mitotic inhibitors on cell cycle progression. *Genes to*
539   *Cells* **2**, 369-380. https://doi.org/10.1046/j.1365-2443.1997.1280326.x
540 Hasegawa, S., Hirashima, N. & Nakanishi, M. (2001) Microtubule involvement in the
541   intracellular dynamics for gene transfection mediated by cationic liposomes. *Gene*
542   *Ther* **8**, 1669-1673. https://doi.org/10.1038/sj.gt.3301573.
543 Ho, Y.K., Zhou, L.H., Tam, K.C. & Too, H.P. (2017) Enhanced non-viral gene delivery
544   by coordinated endosomal release and inhibition of beta-tubulin deactylase.
545   *Nucleic Acids Research* **45**, e38. https://doi.org/10.1093/nar/gkw1143
546 Khalil, I.A., Kogure, K., Akita, H. & Harashima, H. (2006) Uptake pathways and
547   subsequent intracellular trafficking in nonviral gene delivery. *Pharmacol Rev* **58**,
548   32-45. https://doi.org/10.1124/pr.58.1.8
549 Kobayashi, S., Kojidani, T., Osakada, H., Yamamoto, A., Yoshimori, T., Hiraoka, Y. &
550   Haraguchi, T. (2010) Artificial induction of autophagy around polystyrene beads in
551   nonphagocytic cells. *Autophagy* **6**, 36-45. https://doi.org/10.4161/auto.6.1.10324
552 Kobayashi, S., Koujin, T., Kojidani, T., Osakada, H., Mori, C., Hiraoka, Y. &
553   Haraguchi, T. (2015) BAF is a cytosolic DNA sensor that leads to exogenous DNA
554   avoiding autophagy. *Proceedings of the National Academy of Sciences of the*
555   *United States of America* **112**, 7027-7032.
556   https://doi.org/10.1073/pnas.1501235112
557 Kochl, R., Hu, X.W., Chan, E.Y. & Tooze, S.A. (2006) Microtubules facilitate
558   autophagosome formation and fusion of autophagosomes with endosomes. *Traffic*
559   *(Copenhagen, Denmark)* **7**, 129-145. https://doi.org/10.1111/j.1600-
560   0854.2005.00368.x
561 Komatsu, M., Waguri, S., Koike, M. *et al.* (2007) Homeostatic levels of p62 control
562   cytoplasmic inclusion body formation in autophagy-deficient mice. *Cell* **131**, 1149-
563   1163. https://doi.org/10.1016/j.cell.2007.10.035
564 Lim, A.C., Tiu, S.Y., Li, Q. & Qi, R.Z. (2004) Direct regulation of microtubule
565   dynamics by protein kinase CK2. *J Biol Chem* **279**, 4433-4439.
566   https://doi.org/10.1074/jbc.M310563200

567 Lindberg, J., Fernandez, M.A., Ropp, J.D. & Hamm-Alvarez, S.F. (2001) Nocodazole
568   treatment of CV-1 cells enhances nuclear/perinuclear accumulation of lipid-DNA
569   complexes and increases gene expression. *Pharmaceutical Research* **18**, 246-249.
570   https://doi.org/10.1023/a:1011001022570

571 Mackeh, R., Perdiz, D., Lorin, S., Codogno, P. & Pous, C. (2013) Autophagy and
572   microtubules - new story, old players. *Journal of Sell Science* **126**, 1071-1080.
573   https://doi.org/10.1242/jcs.115626

574 Mann, S.S. & Hammarback, J.A. (1994) Molecular characterization of light chain 3. A
575   microtubule binding subunit of MAP1A and MAP1B. *J Biol Chem* **269**, 11492-
576   11497. https://doi.org/10.1016/S0021-9258(19)78150-2

577 Matsumoto, G., Shimogori, T., Hattori, N. & Nukina, N. (2015) TBK1 controls
578   autophagosomal engulfment of polyubiquitinated mitochondria through
579   p62/SQSTM1 phosphorylation. *Human Molecular Genetics* **24**, 4429-4442.
580   https://doi.org/10.1093/hmg/ddv179

581 Matsumoto, G., Wada, K., Okuno, M., Kurosawa, M. & Nukina, N. (2011) Serine 403
582   phosphorylation of p62/SQSTM1 regulates selective autophagic clearance of
583   ubiquitinated proteins. *Molecular Cell* **44**, 279-289.
584   https://doi.org/10.1016/j.molcel.2011.07.039

585 Midoux, P., Breuzard, G., Gomez, J.P. & Pichon, C. (2008) Polymer-based gene
586   delivery: a current review on the uptake and intracellular trafficking of polyplexes.
587   *Curr Gene Ther* **8**, 335-352. https://doi.org/10.2174/156652308786071014

588 Mizushima, N., Yoshimori, T. & Ohsumi, Y. (2011) The role of Atg proteins in
589   autophagosome formation. *Annu Rev Cell Dev Biol* **27**, 107-132.
590   https://doi.org/10.1146/annurev-cellbio-092910-154005

591 Nair, R.R., Rodgers, J.R. & Schwarz, L.A. (2002) Enhancement of transgene expression
592   by combining glucocorticoids and anti-mitotic agents during transient transfection
593   using DNA-cationic liposomes. *Mol Ther* **5**, 455-462.
594   https://doi.org/10.1006/mthe.2002.0567

595 Nakatogawa, H., Suzuki, K., Kamada, Y. & Ohsumi, Y. (2009) Dynamics and diversity
596   in autophagy mechanisms: lessons from yeast. *Nature Reviews. Molecular Cell*
597   *Biology* **10**, 458-467. https://doi.org/10.1038/nrm2708

598   Ogawa, H., Yu, R. T., Haraguchi, T., Hiraoka, Y., Nakatani, Y., Morohashi, K., &
599   Umesono, K. (2004). Nuclear structure-associated TIF2 recruits glucocorticoid
600   receptor and its target DNA. *Biochem Biophys Res Commun* **320**, 218–225.
601   https://doi.org/10.1016/j.bbrc.2004.05.161
602   Pillai, S., Nguyen, J., Johnson, J., Haura, E., Coppola, D. & Chellappan, S. (2015) Tank
603   binding kinase 1 is a centrosome-associated kinase necessary for microtubule
604   dynamics and mitosis. *Nature Communications* **6**, 10072.
605   https://doi.org/10.1038/ncomms10072
606   Polson, H.E., de Lartigue, J., Rigden, D.J., Reedijk, M., Urbe, S., Clague, M.J. &
607   Tooze, S.A. (2010) Mammalian Atg18 (WIPI2) localizes to omegasome-anchored
608   phagophores and positively regulates LC3 lipidation. *Autophagy* **6**, 506-522.
609   https://doi.org/10.4161/auto.6.4.11863
610   Randow, F. (2011) How cells deploy ubiquitin and autophagy to defend their cytosol
611   from bacterial invasion. *Autophagy* **7**, 304-309
612   https://doi.org/10.4161/auto.7.3.14539
613   Rejman, J., Bragonzi, A. & Conese, M. (2005) Role of clathrin- and caveolae-mediated
614   endocytosis in gene transfer mediated by lipo- and polyplexes. *Mol Ther* **12**, 468-
615   474. https://doi.org/10.1016/j.ymthe.2005.03.038
616   Reunanen, H., Marttinen, M. & Hirsimaki, P. (1988) Effects of griseofulvin and
617   nocodazole on the accumulation of autophagic vacuoles in Ehrlich ascites tumor
618   cells. *Exp Mol Pathol* **48**, 97-102. https://doi.org/10.1016/0014-4800(88)90048-2
619   Roberts, R., Al-Jamal, W.T., Whelband, M., Thomas, P., Jefferson, M., van den
620   Bossche, J., Powell, P.P., Kostarelos, K. & Wileman, T. (2013) Autophagy and
621   formation of tubulovesicular autophagosomes provide a barrier against nonviral
622   gene delivery. *Autophagy* **9**, 667-682. https://doi.org/10.4161/auto.23877
623   Rosette, C., & Karin, M. (1995). Cytoskeletal control of gene expression:
624   depolymerization of microtubules activates NF-kappa B. *The Journal of cell*
625   *biology*, **128**, 1111–1119. https://doi.org/10.1083/jcb.128.6.1111
626   Tachibana, K., Yuzuriha, T., Tabata, R. *et al.* (2018) Discovery of peroxisome
627   proliferator-activated receptor alpha (PPARalpha) activators with a ligand-
628   screening system using a human PPARalpha-expressing cell line. *J Biol Chem* **293**,
629   10333-10343. https://doi.org/10.1074/jbc.ra118.002077

630 Tsuchiya, M., Ogawa, H., Koujin, T., Kobayashi, S., Mori, C., Hiraoka, Y. &
631   Haraguchi, T. (2016) Depletion of autophagy receptor p62/SQSTM1 enhances the
632   efficiency of gene delivery in mammalian cells. *FEBS letters* **590**, 2671-2680.
633   https://doi.org/10.1002/1873-3468.12262
634 Tsuchiya, M., Ogawa, H., Koujin, T., Mori, C., Osakada, H., Kobayashi, S., Hiraoka, Y.
635   & Haraguchi, T. (2018) p62/SQSTM1 promotes rapid ubiquitin conjugation to
636   target proteins after endosome rupture during xenophagy. *FEBS Open Bio* **8**, 470-
637   480. https://doi.org/10.1002/2211-5463.12385
638 Vaughan, E.E., Geiger, R.C., Miller, A.M., Loh-Marley, P.L., Suzuki, T., Miyata, N. &
639   Dean, D.A. (2008) Microtubule acetylation through HDAC6 inhibition results in
640   increased transfection efficiency. *Mol Ther* **16**, 1841-1847.
641   https://doi.org/10.1038/mt.2008.190
642 Wang, L. & MacDonald, R.C. (2004) Effects of microtubule-depolymerizing agents on
643   the transfection of cultured vascular smooth muscle cells: enhanced expression
644   with free drug and especially with drug-gene lipoplexes. *Mol Ther* **9**, 729-737.
645   https://doi.org/10.1016/j.ymthe.2004.02.009
646 Wileman, T. (2013) Autophagy as a defence against intracellular pathogens. *Essays in*
647   *Biochemistry* **55**, 153-163. https://doi.org/10.1042/bse0550153
648 Yang, H., Mao, W., Rodriguez-Aguayo, C., Mangala, L.S., Bartholomeusz, G., Iles,
649   L.R., Jennings, N.B., Ahmed, A.A., Sood, A.K., Lopez-Berestein, G., Lu, Z. &
650   Bast, R.C., Jr. (2018) Paclitaxel Sensitivity of Ovarian Cancer Can be Enhanced by
651   Knocking Down Pairs of Kinases that Regulate MAP4 Phosphorylation and
652   Microtubule Stability. *Clin Cancer Res* **24**, 5072-5084.
653   https://doi.org/10.1158/1078-0432.ccr-18-0504
654

655 **Figure legends**

656 **Fig. 1. High-throughput screening for drugs enhancing transfection efficiency**

657 (A) Schematic diagram of the process of high-throughput screening using automated

658 workstations. Murine embryonic fibroblast (MEF) cells were treated with each

659 compound and then transfected with the pCMV-Luc plasmid in the presence of each

660 compound. Cell viability and the luciferase activity from the transfected plasmid were

661 measured. Transfection efficiency was evaluated based on luciferase activity normalized

662 to cell viability. (B) High-throughput screening was performed for 4,400 compounds

663 from the Osaka University compound library as described. Values of transfection

664 efficiency were plotted for the selected 4,240 compounds. Dimethyl sulfoxide (DMSO)

665 was used as the negative control. The red broken line represents the mean $+ 4 \times$ SD of

666 all negative control assay points.

667

668 **Fig. 2. Second screening of compounds selected through high-throughput screening**

669 (A) The top 87 compounds identified in the primary screen were further examined.

670 MEF cells were transfected with the pCMV-Luc plasmid for 28 h in the presence of 1

671 μM of each compound. DMSO was used as the negative control. Transfection efficiency

672 was determined based on luciferase activity normalized to the cell viability. Bar graphs

673 show fold changes in transfection efficiency relative to the value from the control

674 DMSO-treated cells in descending order. The second and third columns represent data

675 for colchicine and vinblastine as indicated. (B) The top 9 potential compounds for

676 enhancement of transfection efficiency. (C) MEF cells were transfected with the

677   pCMV-Luc plasmid for 28 h in the presence of colchicine (left graph) or vinblastine

678   (right graph) at the indicated concentrations. Transfection efficiency was determined as

679   described above. Filled circles and vertical lines indicate the mean and SD, respectively,

680   of at least three independent experiments. (D) Control DMSO-treated MEF cells (a, d),

681   250 nM colchicine-treated MEF cells (b, e), and 50 nM vinblastine-treated MEF cells

682   (c, f) were examined using fluorescence microscopy 24 h after transfection with a GFP-

683   expressing plasmid pCMX-AFAP (upper panels; GFP); the lower panels represent the

684   corresponding bright-field (BF) images of the upper panels. Scale bar = 500 μm.

685

686   **Fig. 3. Colchicine- and vinblastine-treated MEF cells do not enhance transfection**

687   **efficiency in the absence of p62**

688   (A) The top 87 compounds were examined in p62KO-MEF cells. The p62KO-MEF

689   cells were transfected with the pCMV-Luc plasmid for 28 h in the presence of 1 μM of

690   each compound, and transfection efficiency was determined as described in the legend

691   to Fig. 2A. The fold changes in transfection efficiency relative to the value from the

692   control DMSO-treated cells are shown in the same order as in Fig. 2A. The two

693   columns on the right are reproduced from Fig. 2A for comparison. (B, C) The p62KO-

694   MEF cells were transfected for 28 h with the pCMV-Luc plasmid in the presence of the

695   indicated concentrations of colchicine (B) or vinblastine (C). Each value of the

696   transfection efficiency is indicated as the mean ± SD of at least three independent

697   experimental results.

698

29

699 **Fig 4. Colchicine- and vinblastine-treated MEF cells affect the timing of**

700 **ubiquitination**

701 (A) Schematic diagram of the experimental system using beads incorporated into cells

702 to monitor the behavior of transfected materials. (B, C) Time-lapse images of pHrodo

703 and GFP-Ub fluorescence around a single pHrodo-conjugated bead in MEF cells.

704 Images were obtained every minute for approximately 60 min. The panels show

705 representative images of pHrodo and GFP-Ub fluorescence. (B) GFP-Ub MEF cells

706 treated with DMSO as a control. Arrows indicate the timing of appearance of GFP-Ub

707 signals around the beads. (C) GFP-Ub MEF cells treated with 500 nM colchicine.

708 Arrows indicate the timing of appearance of GFP-Ub signals around the beads. Scale

709 bar = 2 μm. (D) Statistical analysis was performed for the time taken for GFP-signal

710 accumulation around the beads after the loss of pHrodo signals in the GFP-Ub MEF

711 cells. Lane 1: control treated with DMSO. Lane 2: 100 nM colchicine-treated MEF

712 cells. Lane 3: 500 nM colchicine-treated MEF cells. Lane 4: 100 nM vinblastine-treated

713 MEF cells. The median values were 4 min for GFP-Ub ($n = 24$ beads), 6 min for 100

714 nM colchicine ($n = 28$ beads), 6 min for 500 nM colchicine ($n = 22$ beads), and 6 min

715 for 100 nM vinblastine ($n = 31$ beads). Three independent experiments were performed

716 for each lane, and the total bead number is indicated as n. Statistical differences ($p <$

717 0.0001) were determined using the Kruskal–Wallis test. Error bars indicate 95%

718 confidence intervals.

719

720 **Fig. 5. Colchicine- and vinblastine-treated MEF cells decrease the level of**

721 **phosphorylated p62 at S405**

722   Western blot analysis was performed for total p62 and S405-phosphorylated p62 in

723   MEF cells. Cells were pretreated with 500 nM colchicine or 100 nM vinblastine for 30

724   min, and then transfected with the pCMX-AFAP plasmid in the presence of 500 nM

725   colchicine or 100 nM vinblastine. DMSO was used as the control. Samples were

726   subjected to Western blot analysis with no transfection or with transfection for 24 h.

727   GAPDH was used as the loading control.

728

Fig. 1

A

B

Fig. 2

A

B

No	chemical name	target	function	PubChem CID
1	PODOFILOX	microtubule	antineoplastic, antimitotic agent	10607
2	COLCHICINE	microtubule	antimitotic, antigout agent	6167
3	VINBLASTINE SULFATE	microtubule	antineoplastic, spindle poison	241902
4	DEOXYSAPPANONE B 7,4'-DIMETHYL ETHER	microtubule		4026888
5	VINCRISTINE SULFATE	microtubule	antineoplastic	249332
6	PICROPODOPHYLLIN ACETATE	microtubule / IGF-1R	antineoplastic	233299
7	DOCETAXEL	microtubule	antineoplastic	148124
8	FENBENDAZOLE	microtubule	anthelmintic, antinematodal drug	3334
9	FLUBENDAZOLE	microtubule	anthelmitic, antinematodal drug	35802

C

D

MEF control [DMSO]   MEF colchicine [250 nM]   MEF vinblastine [50 nM]

GFP

BF

Fig. 3

A

B

C

Fig. 4

A

colchicine or vinblastine

pHrodo-conjugated beads

acidic endosome / pHrodo-conjugated beads

raptured acidic endosome / GFP-Ub

GFP-Ub

GFP-Ubwt MEF cell

B GFP-Ub MEF, DMSO

C GFP-Ub MEF, colchicine 500 nM

D

| over 60 min | 1 | 16 | 3 | 10 |

GFP-Ub accumulation time [min]

$p < 0.0001$

inhibitor treatment: 1 DMSO, 2 100 nM colchicine, 3 500 nM colchicine, 4 100 nM vinblastine

Fig. 5

Supporting Information

Microtubule inhibitors identified through non-biased screening enhance DNA transfection efficiency by delaying p62-dependent ubiquitin recruitment

Megumi Tsuchiya[1#], Hidesato Ogawa[1#]*, Kento Watanabe[1], Takako Koujin[2], Chie Mori[2], Kazuto Nunomura[3], Bangzhong Lin[3], Akiyoshi Tani[3], Yasushi Hiraoka[1,2], and Tokuko Haraguchi[1,2]*

List of contents:
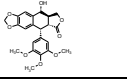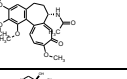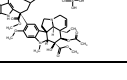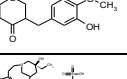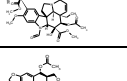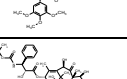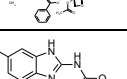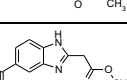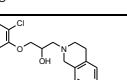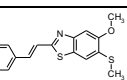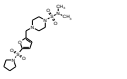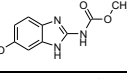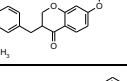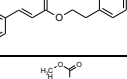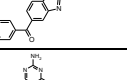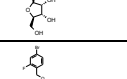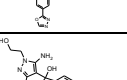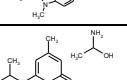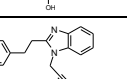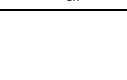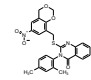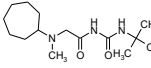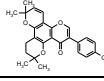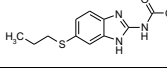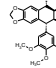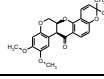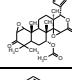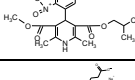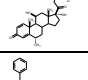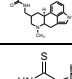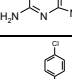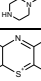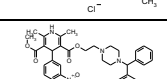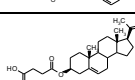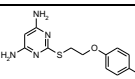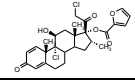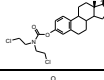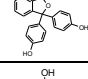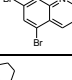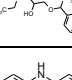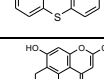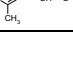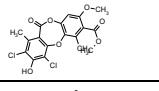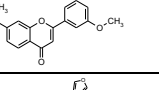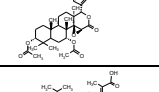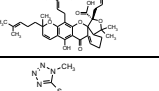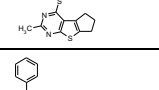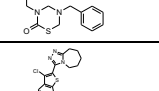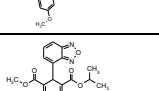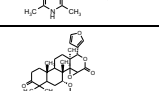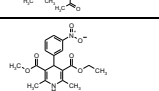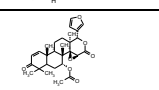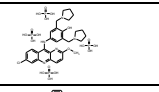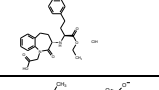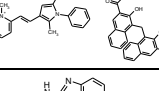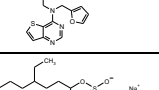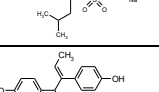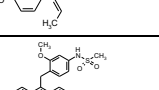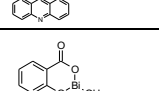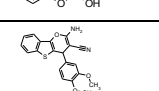
Table S1. Identification of 87 potential compounds for enhancement of transfection efficiency.

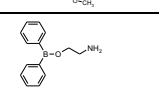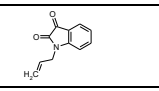| Rank	Structure	Name	Formula	Fold transfection efficiency in MEF	Fold cell viability in MEF	Fold transfection efficiency in p62KO-MEF	Fold cell viability in p62KO-MEF
1		PODOFILOX	C22 H22 O8	297.24	64%	4.46	281%
2		COLCHICINE	C22 H25 N O6	294.20	95%	4.94	258%
3		VINBLASTINE SULFATE	C46 H58 N4 O9 . H2 O4 S	263.07	68%	6.90	318%
4		DEOXYSAPPANONE B 7,4'-DIMETHYL ETHER	C18 H18 O5	54.43	96%	4.72	95%
5		VINCRISTINE SULFATE	C46 H56 N4 O10 . H2 O4 S	46.77	40%	0.66	47%
6		PICROPODOPHYLLIN ACETATE	C24 H24 O9	35.46	34%	2.19	46%
7		DOCETAXEL	C43 H53 N O14 . 3 H2 O	33.78	72%	9.43	316%
8		FENBENDAZOLE	C15 H13 N3 O2 S	27.14	63%	7.83	337%
9		FLUBENDAZOLE	C17 H13 F N2 O3	21.35	71%	4.53	357%
10			C18 H19 Cl F N O2	8.77	59%	1.09	80%
11			C18 H17 N O2 S2	6.80	74%	1.80	68%
12			C15 H26 N4 O5 S2	6.19	89%	1.70	91%
13		OXIBENDAZOLE	C12 H15 N3 O3	4.64	45%	0.85	49%
14		DEOXYSAPPANONE B 7,3'-DIMETHYL ETHER ACETATE	C20 H20 O6	4.50	82%	2.07	85%
15		PHENETHYL CAFFEATE (CAPE)	C17 H16 O4	4.44	72%	1.63	89%
16		MEBENDAZOLE	C16 H13 N3 O3	3.01	95%	1.57	365%
17		AZACITIDINE	C8 H12 N4 O5	2.92	59%	0.93	67%
18			C15 H10 Br F N2 O2	2.84	96%	0.53	109%
19			C15 H18 N4 O3	2.52	97%	0.62	105%
20		PIROCTONE OLAMINE	C14 H23 N O2 . C2 H7 N O	2.04	40%	0.78	42%
21			C18 H16 N2	1.96	94%	0.38	102%

22			C25 H21 N3 O5 S	1.91	113%	0.76	101%
23			C15 H29 N3 O2	1.82	113%	1.52	116%
24		ISOOSAJIN	C25 H24 O5	1.59	62%	1.50	76%
25		ALBENDAZOLE	C12 H15 N3 O2 S	1.50	92%	0.62	222%
26		PICROPODOPHYLLIN	C22 H22 O8	1.49	93%	0.32	110%
27		DEGUELIN(-)	C23 H22 O6	1.44	36%	1.51	33%
28		EPOXYGEDUNIN	C28 H34 O8	1.37	77%	2.66	83%
29		NISOLDIPINE	C20 H24 N2 O6	1.32	91%	1.05	59%
30		METHYLPREDNISOLO NE SODIUM SUCCINATE	C26 H33 O8 . Na	1.30	81%	1.24	65%
31		METERGOLINE	C25 H29 N3 O2	1.29	61%	0.93	54%
32		THIOGUANINE	C5 H5 N5 S	1.28	111%	0.45	106%
33			C11 H15 Cl N2	1.26	76%	1.02	88%
34		TOLONIUM CHLORIDE	C15 H16 N3 S . Cl	1.24	67%	0.49	45%
35		MANIDIPINE HYDROCHLORIDE	C35 H38 N4 O6	1.22	70%	0.90	51%
36		PREGNENOLONE SUCCINATE	C25 H36 O5	1.20	78%	0.85	73%
37			C12 H13 Br N4 O S	1.15	103%	0.56	102%
38		MOMETASONE FUROATE	C27 H30 Cl2 O6	1.14	80%	1.26	54%
39		ESTRAMUSTINE	C23 H31 Cl2 N O3	1.08	71%	0.79	77%
40		PHENOLPHTHALEIN	C20 H14 O4	1.07	76%	0.86	70%
41		BROXYQUINOLINE	C9 H5 Br2 N O	1.07	62%	0.63	58%
42			C19 H30 Cl N O2	1.06	101%	1.04	113%
43		PHENOTHIAZINE	C12 H9 N S	1.05	44%	0.86	64%
44		PEUCENIN	C15 H16 O4	1.05	54%	1.45	31%

45		GANGALEOIDIN	C18 H14 Cl2 O7	1.04	78%	1.71	71%
46		7,3'-DIMETHOXYFLAVONE	C17 H14 O4	1.01	84%	1.43	96%
47		3-ACETYLGEDUNOL	C30 H40 O8	1.00	102%	1.37	96%
48		GARCINOLIC ACID	C38 H46 O9	0.99	62%	0.88	54%
49			C12 H12 N6 S2	0.97	109%	0.94	126%
50		SULBENTINE	C17 H18 N2 O S	0.92	72%	0.63	73%
51			C16 H16 Cl N3 O S	0.92	85%	0.85	95%
52		ISRADIPINE	C19 H21 N3 O5	0.90	91%	0.80	71%
53		DIHYDROGEDUNIN	C28 H36 O7	0.90	37%	1.23	69%
54		NITRENDIPINE	C18 H20 N2 O6	0.88	72%	0.82	72%
55		GEDUNIN	C28 H34 O7	0.87	54%	1.23	80%
56		PYRONARIDINE TETRAPHOSPHATE	C29 H32 Cl N5 O2 . 4 H3 O4 P	0.87	79%	0.83	66%
57		BENAZEPRIL HYDROCHLORIDE	C24 H28 N2 O5 . Cl H	0.86	76%	1.06	60%
58		PYRVINIUM PAMOATE	C26 H28 N3 . C23 H15 O6	0.85	79%	1.46	147%
59			C12 H12 N4 S	0.83	101%	0.70	105%
60			C16 H13 N3 O S2	0.82	129%	0.80	137%
61		SODIUM TETRADECYL SULFATE	C14 H29 O4 S . Na	0.81	76%	0.83	69%
62		DIENESTROL	C18 H18 O2	0.81	92%	0.61	219%
63		AMSACRINE	C22 H20 N2 O3 S	0.81	38%	0.18	35%
64		BISMUTH SUBSALICYLATE	C7 H5 Bi O4	0.78	84%	0.84	48%
65			C20 H16 N2 O3 S	0.78	94%	0.86	104%
66		AMINOETHOXYDIPHENYLBORANE	C14 H16 B N O	0.76	94%	0.88	96%
67			C11 H9 N O2	0.75	97%	0.69	106%

68		OXFENDAZOLE	C15 H13 N3 O3 S	0.73	77%	0.80	78%
69		CHLOROXINE	C9 H5 Cl2 N O	0.71	87%	0.72	80%
70		DIETHYLSTILBESTROL	C18 H20 O2	0.66	105%	0.45	204%
71		ESTRADIOL ACETATE	C20 H26 O3	0.60	28%	1.21	49%
72			C23 H26 O3	0.55	104%	0.81	97%
73			C22 H17 N3 O3	0.44	110%	0.86	99%
74			C15 H18 N4 O3 S3	0.41	14%	7.11	37%
75			C14 H14 N4 O S3	0.07	203%	2.33	265%
76			C15 H10 F3 N3 S	0.07	257%	2.35	270%
77			C15 H17 N3 O3	0.07	199%	2.67	260%
78			C16 H10 Br Cl2 N5	0.06	203%	2.62	257%
79			C20 H23 N O4 S	0.06	203%	1.80	265%
80			C17 H10 Cl N O4	0.06	206%	2.52	262%
81			C17 H19 Br O3	0.06	222%	2.36	268%
82			C15 H13 Cl N2 O4 S	0.05	164%	1.75	155%
83			C15 H14 Cl N3 O	0.04	171%	1.52	163%
84			C16 H13 Cl N4 O S2 . Cl H	0.04	186%	1.59	162%
85			C15 H13 Br N2 O2 S	0.03	152%	1.58	150%
86			C14 H18 N6 O2 S	0.03	182%	1.26	190%
87			C16 H18 N2 O2	0.03	203%	1.27	188%

Comparison of 87 compounds derived from the Osaka University compound library, showing their chemical structure, name, formula, transfection efficiency and cell viability in MEF cells and p62KO-MEF cells.
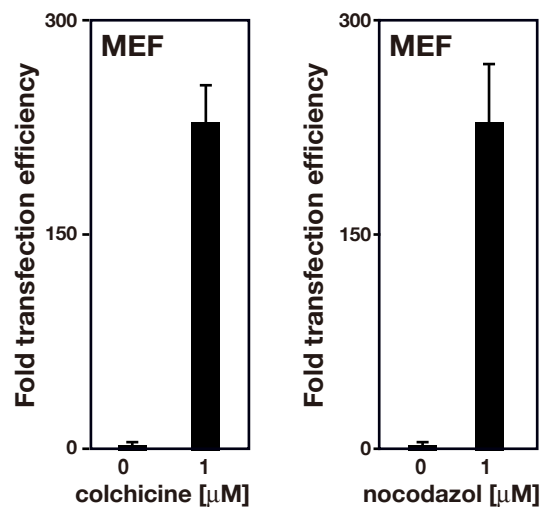
Fig. S1. Nocodazole increases gene transfection efficiency.

MEF cells were transfected with the pCMV-Luc plasmid for 28 h in the presence of 1 μM colchicine (left) and 1 μM nocodazole (right). DMSO was used as the negative control. Transfection efficiency was determined based on luciferase activity normalized to the cell viability. Bar graphs show the fold changes in transfection efficiency relative to the value from the control DMSO-treated cells. Each value is indicated as the mean ± SD of at least threeindependent experiments.
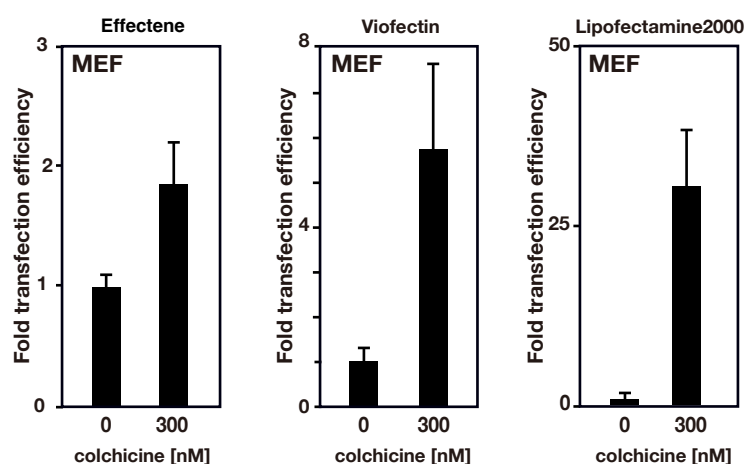
Fig. S2. Colchicine increases transfection efficiency for various transfection reagents.

MEF cells were transfected with the pCMV-Luc plasmid in the presence of 300 nM colchicine by using Effectene, Viofectin, or Lipofectamine 2000. DMSO was used as the negative control. Details of transfection procedures for each transfection reagent are described in the Experimental procedures. Bar graphs show the fold changes in transfection efficiency relative to the value from the control DMSO-treated cells. (mean ± SD of at least three independent experiments).
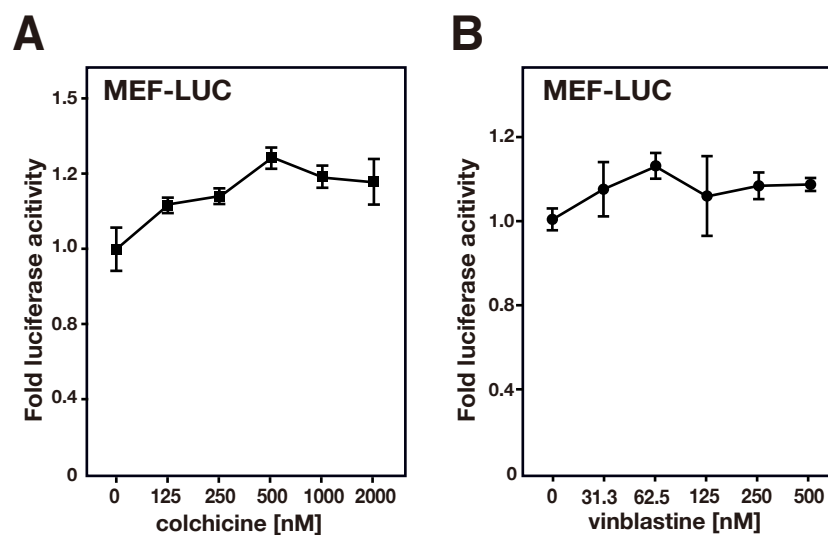
Fig. S3. Colchicine and vinblastine treatments do not affect the promoter activity of the luciferase gene.

(A, B) MEF cells stably expressing luciferase (MEF-LUC) were treated with the indicated concentrations of colchicine (A) or vinblastine (B). After incubation for 27 h, the luciferase activity of the cells was measured and normalized to cell viability. The graphs show the fold changes in luciferase activity relative to the value from the control DMSO-treated cells (indicated as mean ± SD of at least three independent experimental results).